Improved detection algorithms for low-frequency MHD activity in NSTX

Josh Kallman, PPPL

Advisor: Jonathan Menard, PPPL

Overview

- Motivation – Introduction to NSTX and MHD instabilities
- Prior methods of mode detection and correction
- Development of an advanced algorithm; results
- Conclusions and future work

MHD Instabilities and Error Fields

- Global MHD instabilities can limit β in NSTX plasmas and lead to loss of confinement
  - Instabilities can also be created or enhanced by the error fields present in NSTX
- Passive stabilization can be achieved by plasma rotation and electrically conducting plates
- Static error fields occur in NSTX due to non-axisymmetric magnetic fields
  - In particular, the TF coils undergo a significant force and shift position slightly during the course of a shot, causing error fields and leading to locked modes
  - These locked modes can exert a torque on the plasma and slow its rotation

The Resistive Wall Mode

- The RWM is a kink mode modified by the presence of a conducting wall
  - Once plasma rotation falls below Ω_{crit}, a kink mode can grow, which itself rotates at 50 – 100 Hz
  - This can lead to a further loss of rotation and β collapse on the order of the wall eddy current decay time, with a growth rate of 1-10 ms
  - Generally, the most important mode of the instability is the n = 1 mode
  - At high values of β_N, higher order modes, n = 2, n = 3 can also become unstable
- In addition, the error fields in NSTX can lead to magnetic island formation, which can then become amplified and lock as the plasma rotation slows due to the presence of the RWM

The RWM in NSTX

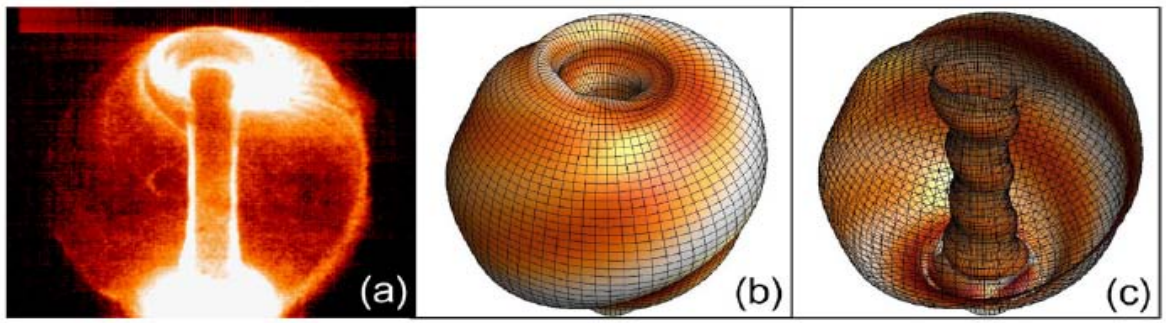

Figure 4. Visible light emission (*a*) and DCON computed normal perturbed field (*b*) and (*c*) for the unstable RWM shown in figure 3(*a*). (discharge 114147) at $t = 0.268$ s.

S.A. Sabbagh, et al. Nucl. Fusion **46** (2006) 638

- These instability magnitude has been multiplied by a factor of 10 to aid in visibility
- The external mode essentially 'rides' on top of the plasma edge, and since the plasma rotation frequency is much greater than the mode rotation frequency, it sees the mode as rotating in reverse and exerting a torque on the plasma, which slows its rotation
- This is a non-linearly instable feedback loop, as the reduced plasma rotation causes the instability grow even faster

Mode detection

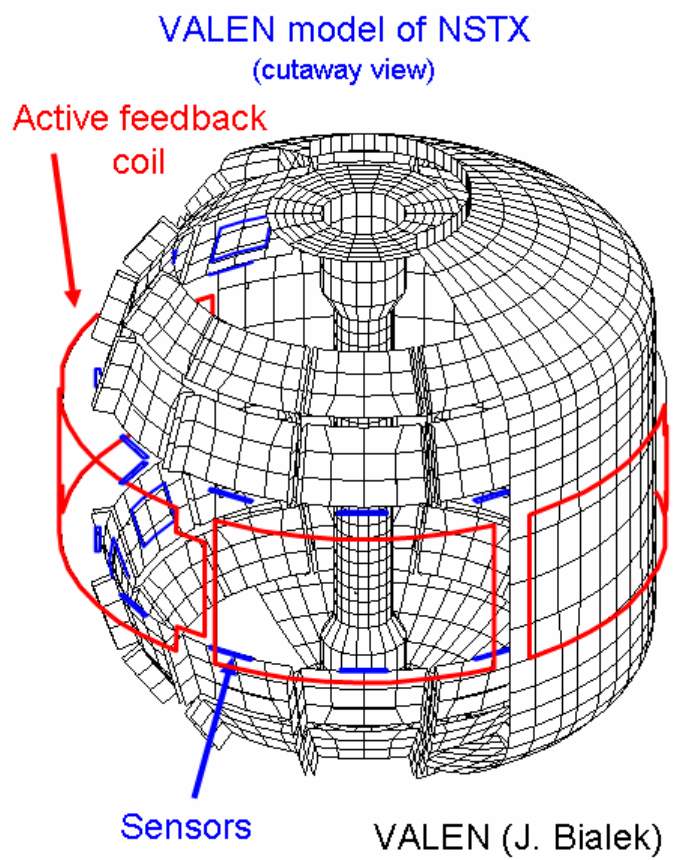

- 24 poloidal and 24 radial internal sensors
- 12 upper and 12 lower for each group divided into 6 pairs
- Inductive wire loops that measure the difference in magnetic flux through the two sensors in the pair

A possible solution: feedback coils

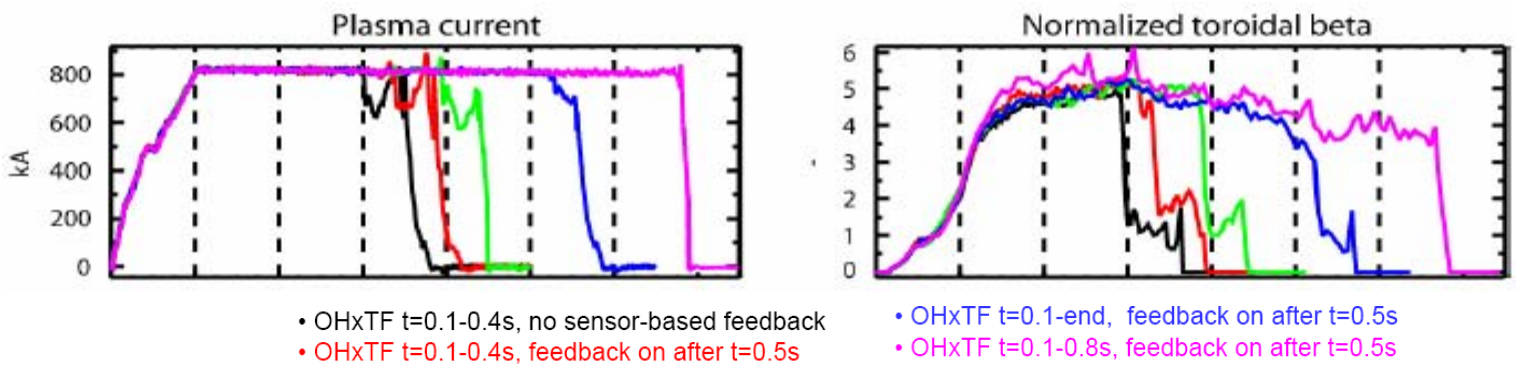

- The NSTX feedback coils are capable of generating an n=1 field with arbitrary phase in order to counteract error field modes
- This feedback has been shown to allow increased operation at high β

How we use the data for feedback

- We have 6 sensor pairs for each group (i.e. upper poloidal)
- We want to solve for the amplitudes and phases for the n = 1,2, and 3 modes (even though feedback is only on n=1)
- We need an relation between our real data and the theoretical structure of the B field which we can then use to solve for the mode characteristics

Sinusoidal representation of the B field for algorithm input

- The perturbed B field can be represented as a truncated Fourier series in toroidal angle φ

$$B(\phi, t) = \sum_n A_n(t) \cos(n\phi - \Phi_n(t))$$

- The phase Φ represents the position of the mode in the machine, and is allowed to vary in time
- We then take *m* measurements, where φ_m is the toroidal position of the different sensors
- In order to subtract off the n = 0 baseline component of the field, we take the difference of the field at different sensor positions

B field in matrix form

$$B_k = \sum_n A_n [s_{kn} \sin(n\Phi_n) + c_{kn} \cos(n\Phi_n)]$$

$$c_{kn} \equiv \cos(n\phi_l) - \cos(n\phi_m) \qquad s_{kn} \equiv \sin(n\phi_l) - \sin(n\phi_m)$$

$$\begin{bmatrix} B_1 \\ B_2 \\ . \\ . \\ . \\ B_M \end{bmatrix} = \begin{bmatrix} s_{10} & s_{11} & . & . & s_{1N} & c_{10} & c_{11} & . & . & c_{1N} \\ . & . & & & . & . & . & & & . \\ . & . & & & . & . & . & & & . \\ . & . & & & . & . & . & & & . \\ . & . & & & . & . & . & & & . \\ s_{M0} & s_{M1} & . & . & s_{MN} & c_{M0} & c_{M1} & . & . & c_{MN} \end{bmatrix} \begin{bmatrix} A_1 \sin(\Phi_1) \\ . \\ A_N \sin(\Phi_N) \\ A_1 \cos(\Phi_1) \\ . \\ A_N \cos(\Phi_N) \end{bmatrix}$$

Solving for the n-modes of the instabilities

- Measurements are separated into radial and poloidal data and then further into upper and lower, and then solved separately
- Once the equation is in matrix form, a method called Singular Value Decomposition (SVD) is employed
- This is a linear algebra method we employ numerically to calculate the pseudo-inverse of the sin/cos matrix[1]
- By then multiplying both sides by this equation, we can isolate the amplitude and phase matrix, which contains the time dependent state of the perturbation

$$\begin{bmatrix} A_1 \sin(\Phi_1) \\ . \\ A_N \sin(\Phi_N) \\ A_1 \cos(\Phi_1) \\ . \\ A_N \cos(\Phi_N) \end{bmatrix} = \begin{bmatrix} \alpha_1 \\ . \\ \alpha_N \\ \beta_1 \\ . \\ \beta_N \end{bmatrix}$$

$$A_n = [\alpha_n^2 + \beta_n^2]^{1/2} \qquad \tan\Phi_n = \frac{\alpha_n}{\beta_n}$$

1 See **Press, W., Flannery, B., Teukolsky, S., & Vetterling, W. (1989).** ***Numerical recipes in C: The art of scientific computing*****. Cambridge: Cambridge University Press. p59**

Instability visualization

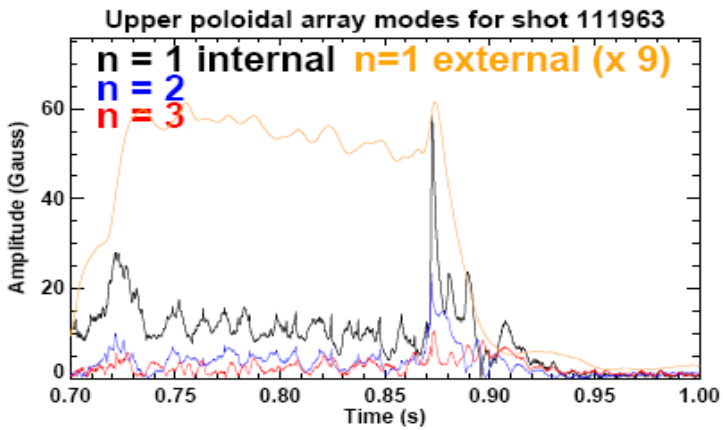

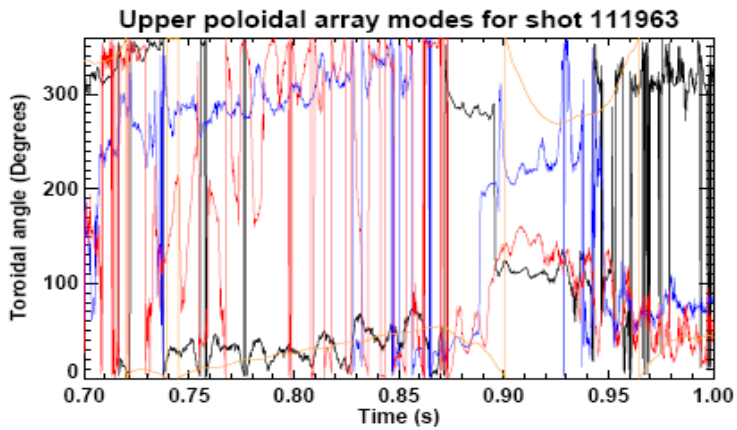

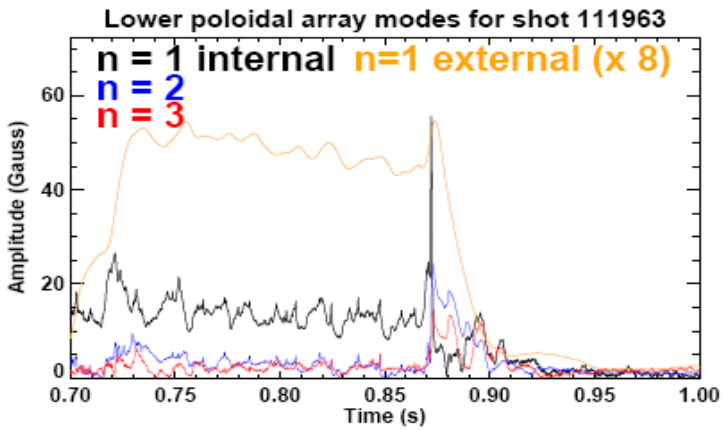

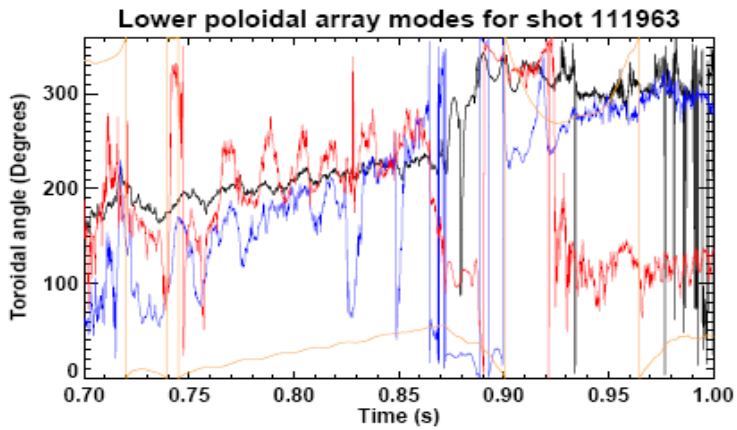

The problems of a real system – sensor death

- NSTX routinely undergoes a “bake out” procedure to reduce impurity levels on plasma-facing components
  - The components are heated to 400° C, which can distort the sensor loops and make them inoperable
  - Plasma interaction with facing components as well as EM forces on the sensor loops can also impact sensor function
- Since we are solving for 3 modes, we have 2n unknowns and 6 equations
  - With sensor death, however, the problem becomes under-constrained
  - A solution can still be found, but the phase and amplitude values of the modes will generally be inaccurate
  - The degree of inaccuracy depends on which sensor pairs are missing

A note on sensor placement

Sensor pair locations (toroidal degrees):

1: 30, 210
2: 120,300
3: 60, 150
4: 90, 180
5: 240, 330
6: 270, 360

Sensors are at the same toroidal locations in the top and bottom halves of the machine.

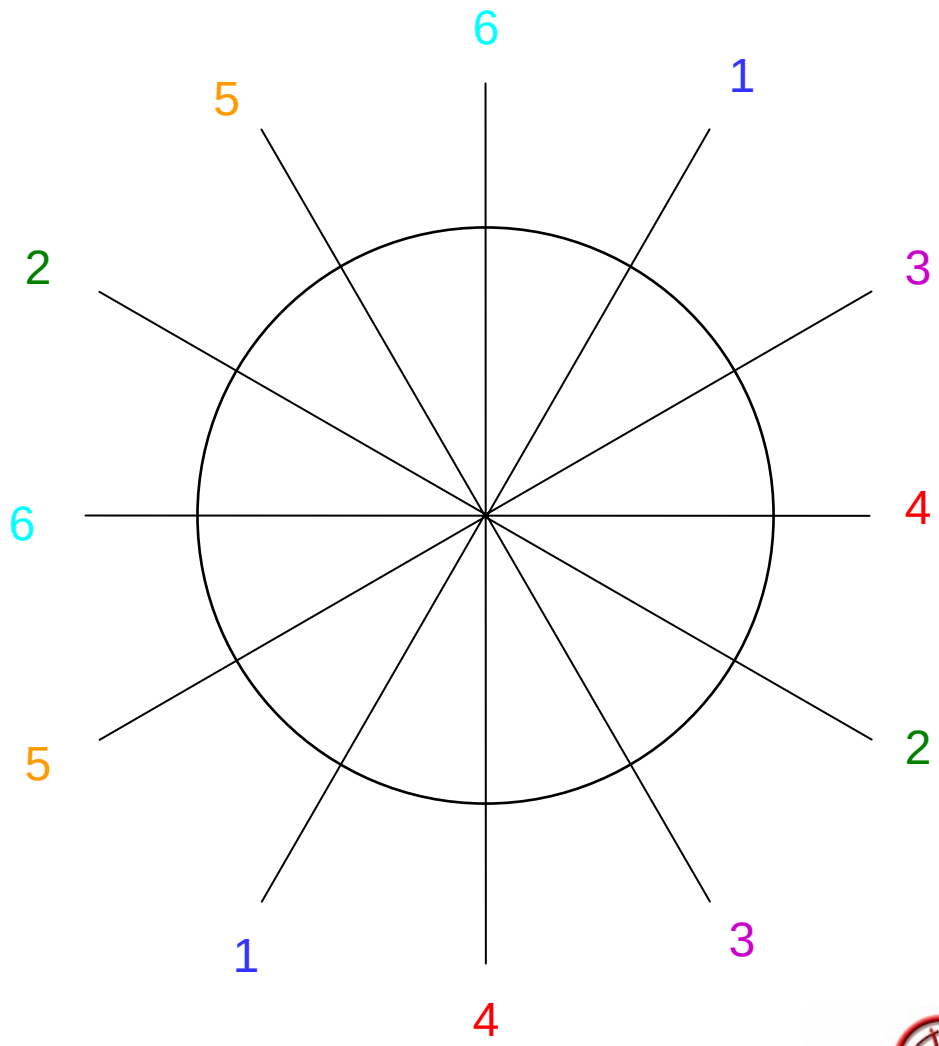

The effect of missing sensors on phase angle

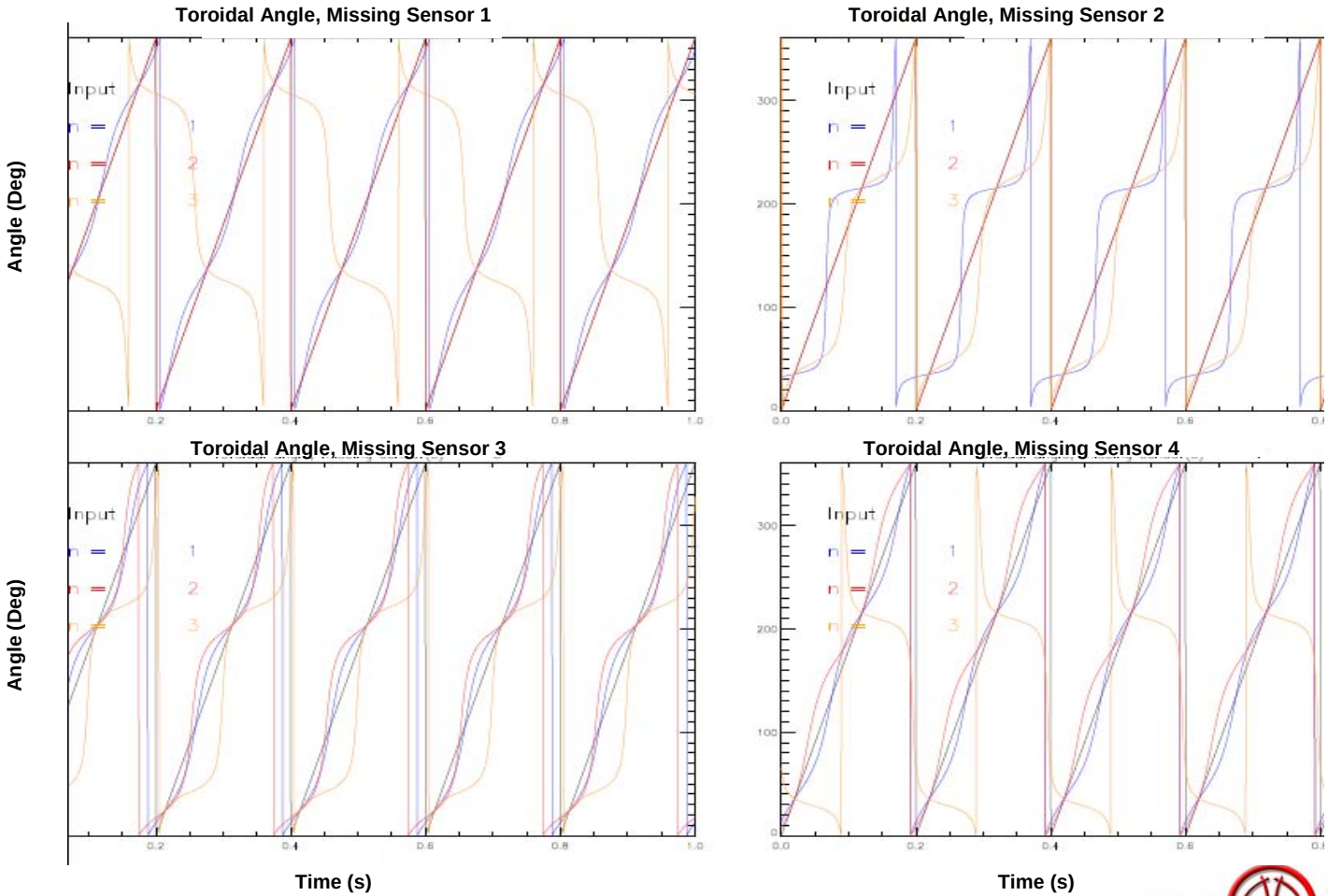

More effects (2 missing sensor pairs)

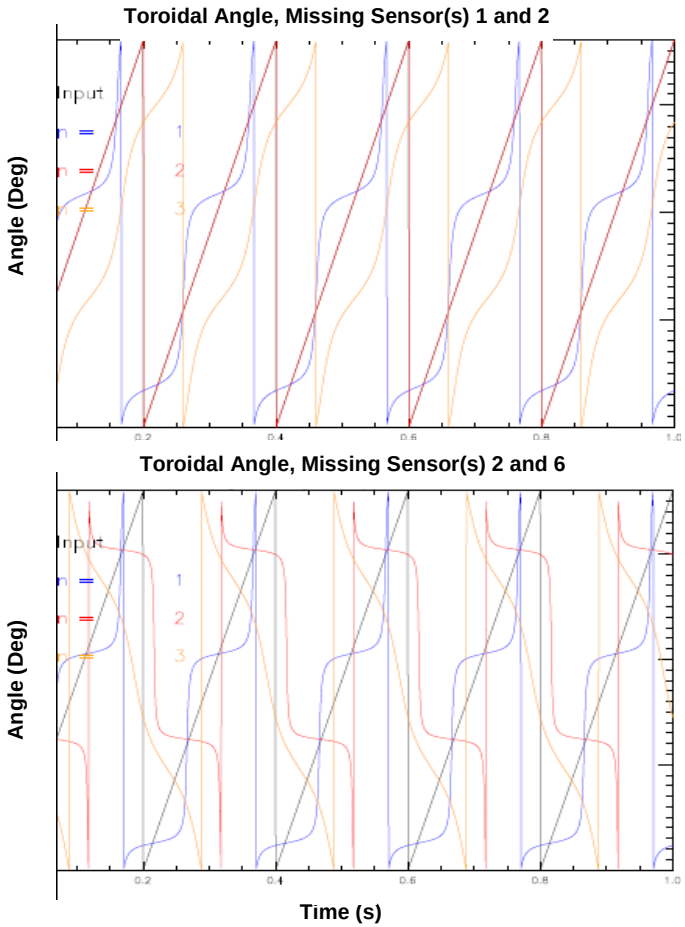

Effects of missing sensors on average amplitude

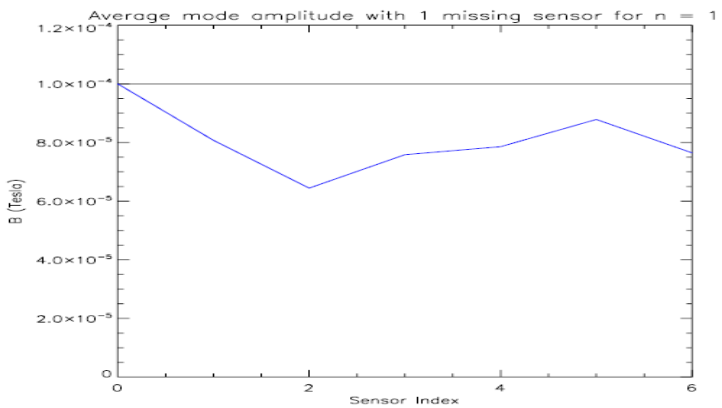

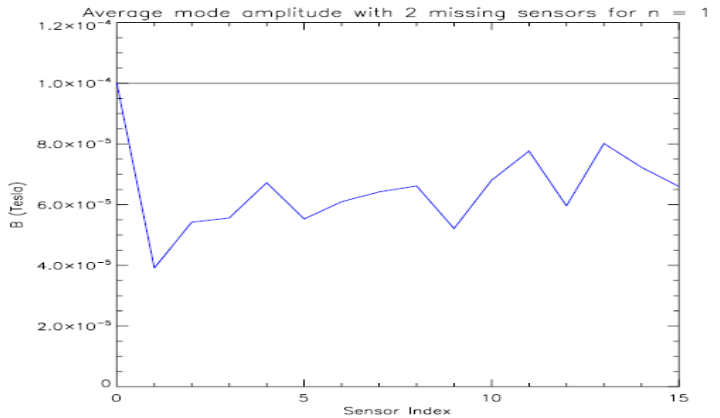

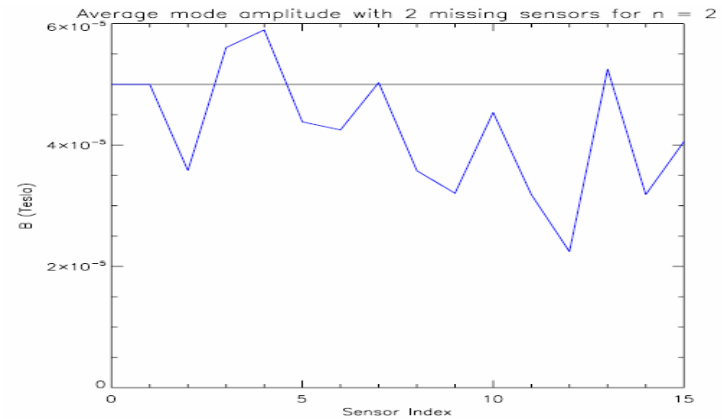

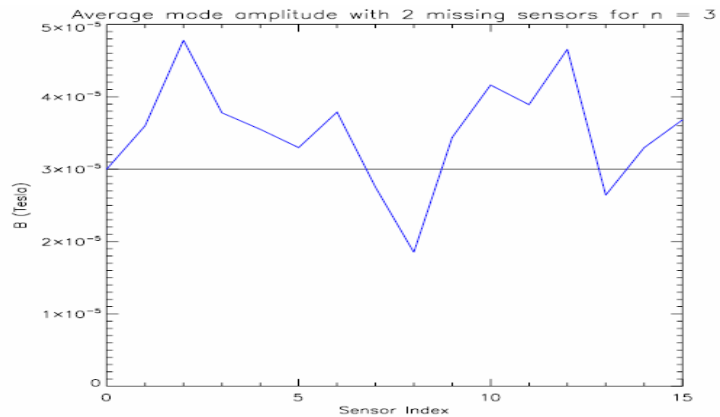

The need for an advanced algorithm

- In order to do real time feedback, the mode must be accurately detected as it begins its growth
  - As shown above, various missing sensors can cause errors in the way a mode is perceived by the old algorithm
  - Often, a mode might be detected by the upper or lower sensor arrays but not both
- Since n = 1 goes as sin(φ), we have only one period spanning the entire machine
  - If we lose pairs 1 or 2 (or both), we lose the 180° separation data for the mode, and thus the maximum amplitude cannot be as accurate as if the data were present
- The feedback coils are located at the midplane of the machine, so it would be beneficial to figure out the mode characteristics at that position in order to feed back most effectively on the mode

Advanced algorithm assumptions

- If we refer back to our assumption that the mode is a sinusoidal perturbation, one can see that the phase will differ in the upper and lower hemitoroids
- We then assume a constant phase shift Φ between the modes, which is often justified when the mode locks, with each mode differing by half of this constant shift

$$\Phi_U = -\frac{\Phi}{2} \qquad \Phi_L = \frac{\Phi}{2}$$

- We do not need to make any assumptions about the amplitude relation between the upper and lower portions of the mode, as the SVD solver will handle this

An attempt at midplane δB calculation

- The transition in the new solution matrix is relatively straightforward, as the shifted phase is accomplished by telling the algorithm that the sensor positions are shifted by either Φ_U or Φ_L
- For example, sensor pair 1 for the upper array is normally at 30 ° and 120 °, but at $\Phi = 60°$, they would be effectively located at 0° and 90°, while the lower sensor pair 1 would be at 60° and 150°
- Now we have introduced more equations into the problem, so a missing sensor pair or two will not reduce the problem to an under- constrained one
- The method for determining the amplitudes and phases for the modes is the same as before, so the code does not have to be modified in a significant way to accommodate this change

New SVD matrix

- This method changes the s_{kl} and c_{kl} elements of the matrix, which now concatenates the upper and lower sensor measurements to solve for the amplitudes and phases of the modes

$$\begin{bmatrix} B_{1U} \\ B_{2U} \\ \cdot \\ \cdot \\ B_{MU} \\ B_{1L} \\ B_{2L} \\ \cdot \\ \cdot \\ B_{ML} \end{bmatrix} = \begin{bmatrix} s^U_{10} & s^U_{11} & \cdot & \cdot & s^U_{1N} & c^U_{10} & c^U_{11} & \cdot & \cdot & c^U_{1N} \\ \cdot & \cdot & & & \cdot & \cdot & \cdot & & & \cdot \\ \cdot & \cdot & & & \cdot & \cdot & \cdot & & & \cdot \\ \cdot & \cdot & & & \cdot & \cdot & \cdot & & & \cdot \\ \cdot & \cdot & & & \cdot & \cdot & \cdot & & & \cdot \\ s^U_{M0} & s^U_{M1} & \cdot & \cdot & s^U_{MN} & c^U_{M0} & c^U_{M1} & \cdot & \cdot & c^U_{MN} \\ s^L_{10} & s^L_{11} & \cdot & \cdot & s^L_{1N} & c^L_{10} & c^L_{11} & \cdot & \cdot & c^L_{1N} \\ \cdot & \cdot & & & \cdot & \cdot & \cdot & & & \cdot \\ \cdot & \cdot & & & \cdot & \cdot & \cdot & & & \cdot \\ \cdot & \cdot & & & \cdot & \cdot & \cdot & & & \cdot \\ \cdot & \cdot & & & \cdot & \cdot & \cdot & & & \cdot \\ s^L_{M0} & s^L_{M1} & \cdot & \cdot & s^L_{MN} & c^L_{M0} & c^L_{M1} & \cdot & \cdot & c^L_{MN} \end{bmatrix} \begin{bmatrix} A_1 \sin(\Phi_1) \\ \cdot \\ A_N \sin(\Phi_N) \\ A_1 \cos(\Phi_1) \\ \cdot \\ A_N \cos(\Phi_N) \end{bmatrix}$$

Calibration and testing

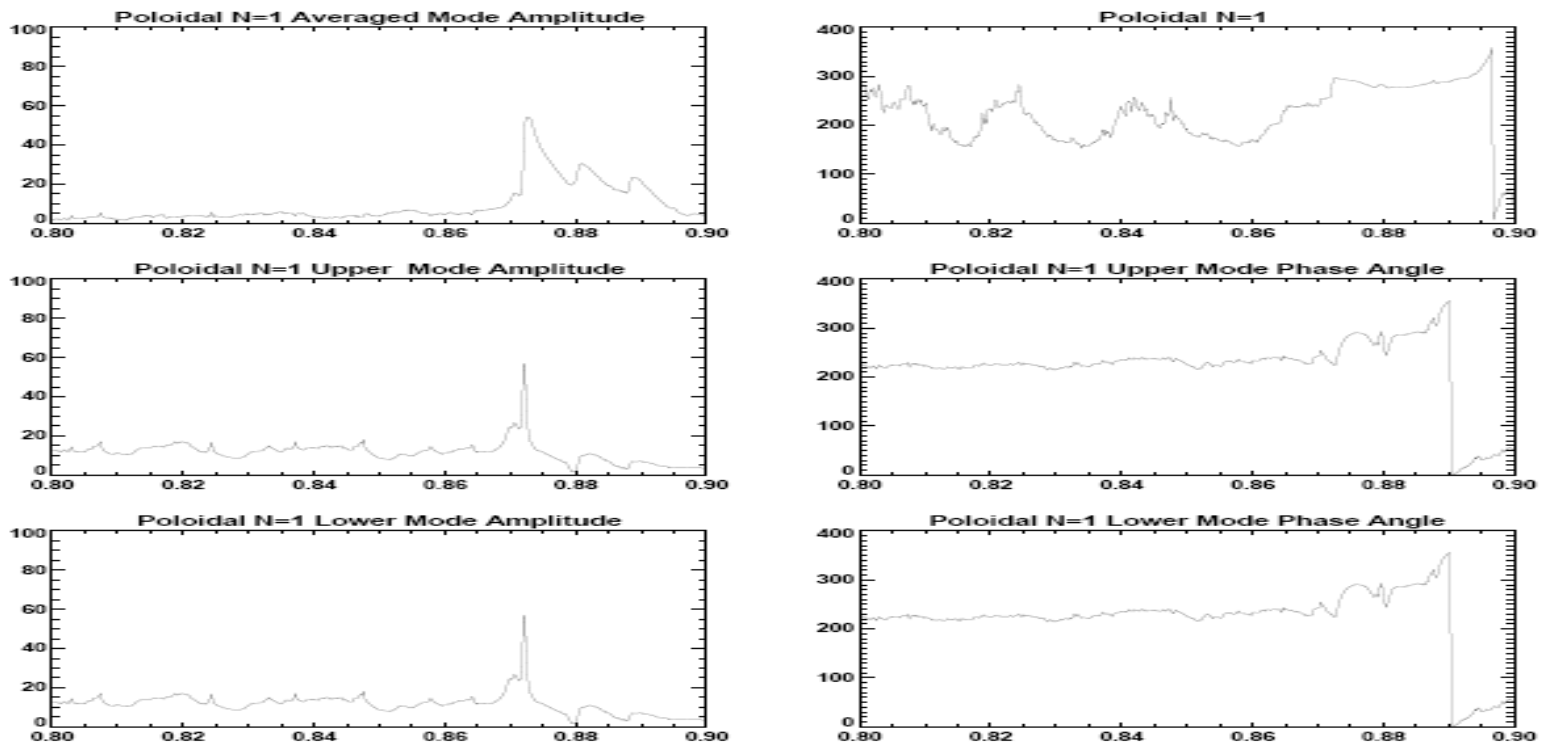

Shot = 111963

Shot analysis, 120669

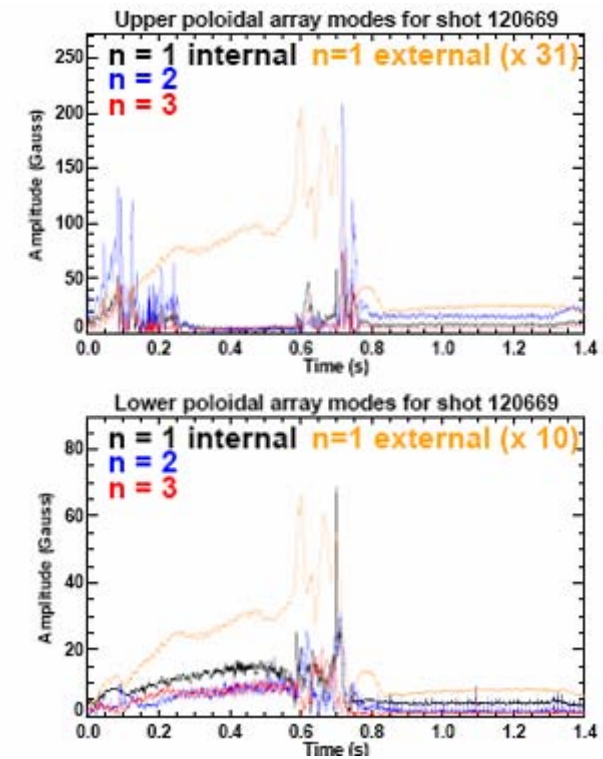

Modes from old algorithm, missing upper sensor pair 4 and lower sensor pair 3

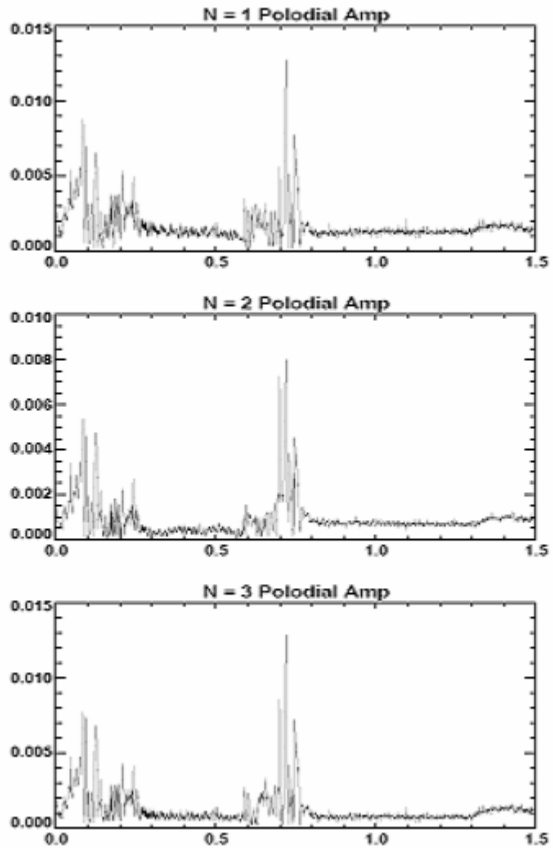

Modes from new algorithm, phase shift assumed 150°

Optimum phase angle studies

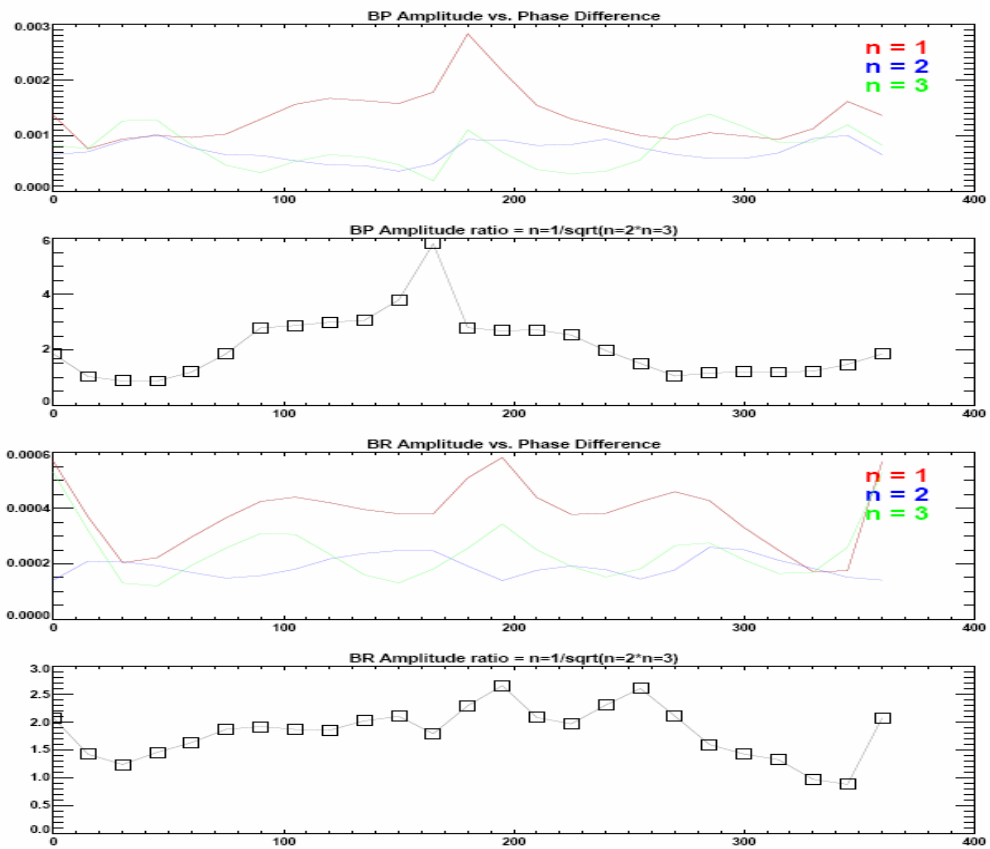

Shot = 120669

Comparison to old algorithm with synthetic data and same missing sensors as 120669, n=1 case

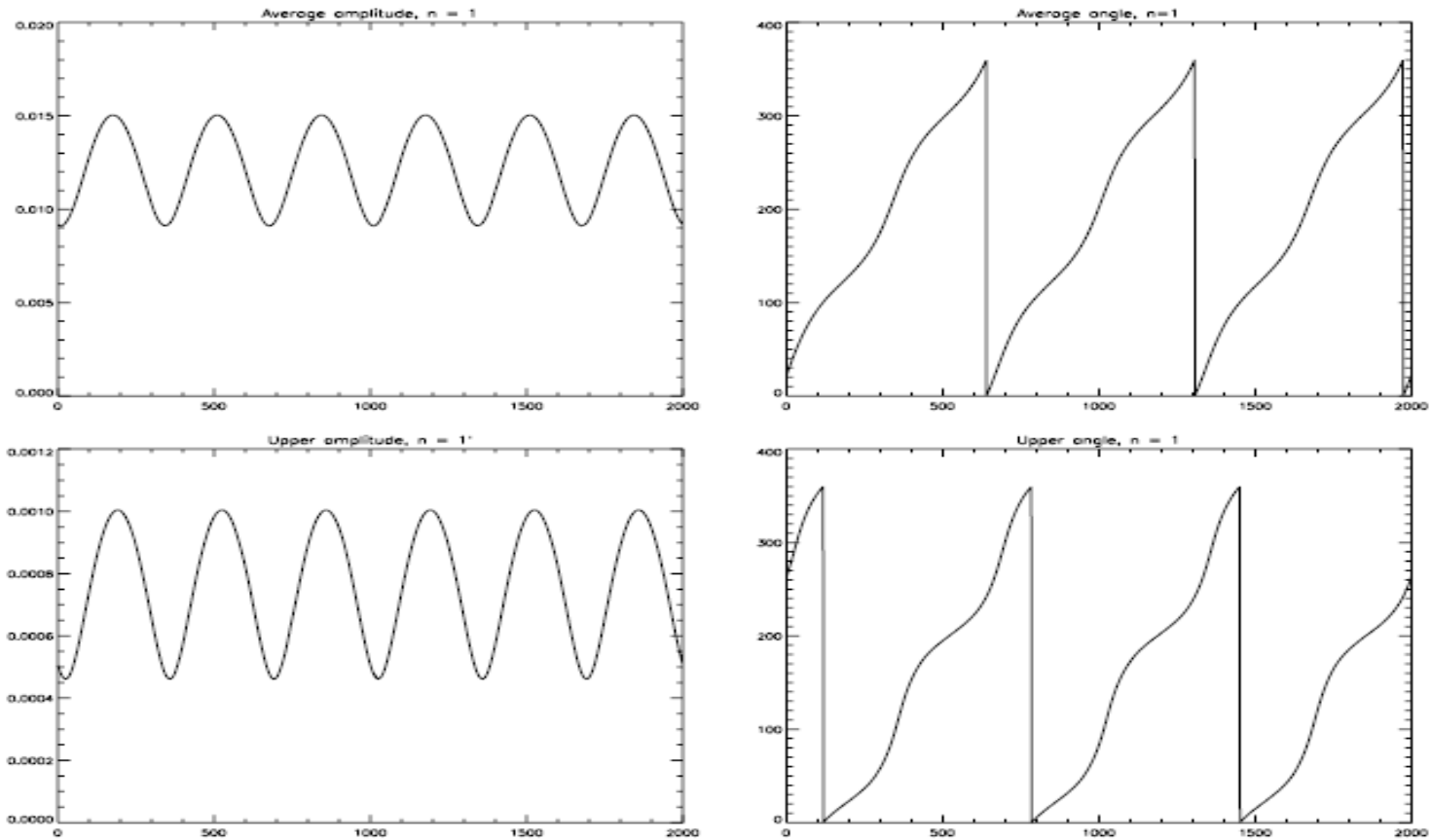

Comparison to old algorithm with synthetic data and same missing sensors as 120669, n=2 case

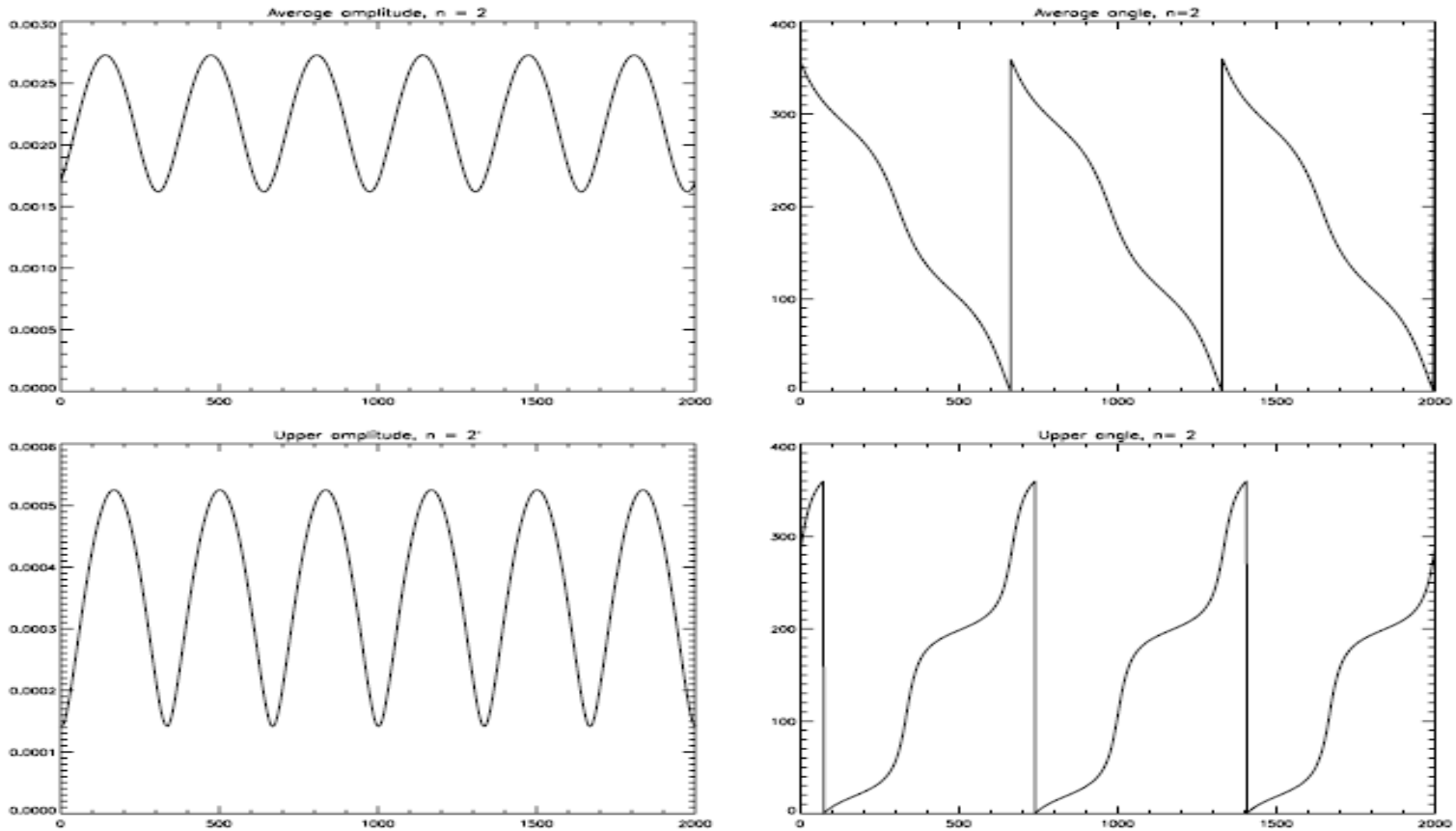

Conclusions

- The averaging algorithm is successful in that it can synthesize the important features of both the upper and lower sensor arrays
- There are some situations where the algorithm has difficulty (especially with n = 2)
- Since we're only able to feedback on n=1, and are able to get a better picture of this with the averaging algorithm, it is useful for the system currently in place

Plans for future implementation

- The algorithm needs to be tested in real time to see if it proves effective
- A constant phase shift between the upper and lower modes is not always realistic, and this could be compensated for in the new code
- A further averaging of both the poloidal and radial modes can be attempted, going for even greater accuracy in the face of sensor failure